

Ran Zheng,^a Lei Han,^b Qinhe Pan,^c Kirsten E. Christensen^{d*} and Tiezhen Ren^{a*}

^aHebei University of Technology, People's Republic of China, ^bStockholm University, Sweden, ^cHaiNan University, People's Republic of China, and ^dUniversity of Oxford, England

Correspondence e-mail:
kirsten.christensen@chem.ox.ac.uk,
rtz@hebut.edu.cn

Two novel Zn-MOFs: structures and characterization

Received 2 December 2011

Accepted 22 February 2012

Two novel three-dimensional Zn-MOFs (zinc metal-organic frameworks), $Zn_5(\mu_3\text{-OH})(\text{BTC})_3(\text{Phen})_4 \cdot 5\text{H}_2\text{O}$ (denoted as HUT-11) and $Zn_4(\mu_4\text{-O})(\text{BTC})_2(\text{Phen})_2 \cdot 4\text{H}_2\text{O}$ (denoted as HUT-12), have been synthesized by metal–ligand-directed assembly under hydrothermal conditions. Here, BTC and Phen are denoted as 1,3,5-benzenetricarboxylate and phenanthroline. HUT-11 contains two kinds of secondary building units (SBUs), $Zn_3(\mu_3\text{-OH})(\text{COO})_5$ clusters and $Zn_2(\text{COO})_4$ clusters. This material exhibits a new three-dimensional (3,4,5)-connected topology with the Schläfli symbol $(4\cdot6\cdot8)_2(4\cdot8^2)(4\cdot6^4\cdot8^5)(4^2\cdot6^2\cdot8^2)$. Two perpendicular planes cross at five coordinated Zn1–Zn3–Zn5 nodes, giving a new three-dimensional network. HUT-12 is composed of $Zn_4(\mu_4\text{-O})(\text{COO})_6$ clusters as the secondary building units and displays a two-dimensional (3,6)-connected TiS_2 related net topology with the Schläfli symbol $(4^2\cdot6)(4^4\cdot6^2\cdot8^8\cdot10)$. Both MOFs show blue light emission and a high thermal stability above 673 K.

1. Introduction

Metal-organic frameworks (MOFs), with flexible pore structure and advanced properties, have attracted much attention (Rosi *et al.*, 2005). The design and synthesis of MOFs not only break the limitation of traditional structures, but also provide interesting materials with effectively low density and high surface area. Clusters of metal cations in connection with functional groups of carboxylate or pyridine give the SBUs, which assemble into two- or three-dimensional crystal structures (Cui *et al.*, 2005). Multinuclear metal clusters including a wide range of metals, from transition metals to rare-earth metals, have been applied for the formation of novel architectures. In the case of Zn^{II} , SBUs from dinuclear to octanuclear have been reported (Fang *et al.*, 2007; Li *et al.*, 2007).

The design and controlled arrangement of organic linkers based on metal clusters and ligands can influence the crystal structure formed in the hydrothermal system, for example by means of the coordination nature of metal ions, the symmetry of organic ligands and the template effect of the synthesis. So far, aromatic polycarboxylate ligands (Forster *et al.*, 2005; Cheetham *et al.*, 2006) have been extensively used in the preparation of various MOFs. However, single ligands restrict the number of new MOF structures which are accessible and therefore binary systems have received more attention in recent years. There are several reports about the binary ligands system based on 1,3,5-benzenetricarboxylic acid (H3BTC) and phenanthroline (Phen) with Zn^{II} ions, which have shown promise for the construction of open frameworks. Concerning the sensitive hydrothermal conditions and synthesis protocol, the formation of the SBUs is still in question.

Table 1

Summary of crystal data and structure refinements for HUT-11 and HUT-12.

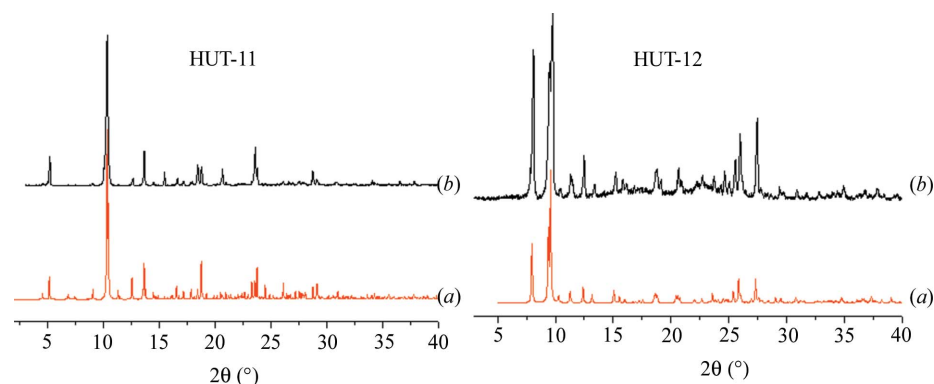
 For all structures: monoclinic, $C2/c$. Refinement was with 0 restraints.

	HUT-11	HUT-12
Crystal data		
Chemical formula	$C_{75}H_{42}N_8O_{19}Zn_5 \cdot H_2O \cdot 3.04O$	$C_{42}H_{22}N_4O_{13}Zn_4 \cdot 5O_{0.50}$
M_r	1752.73	1116.12
Temperature (K)	150	293
a, b, c (Å)	33.057 (3), 23.8834 (17), 17.1688 (12)	15.4925 (4), 15.6741 (6), 17.0388 (3)
β (°)	90.0890 (10)	92.353 (3)
V (Å ³)	13924.0 (19)	4134.1 (2)
Z	8	4
Radiation type	Synchrotron, $\lambda = 0.6889$ Å	Mo $K\alpha$
μ (mm ⁻¹)	1.64	2.38
Crystal size (mm)	0.04 × 0.03 × 0.03	0.24 × 0.20 × 0.20
Data collection		
Diffractometer	Rigaku Saturn724+ (2x2 bin mode)	Xcalibur
Absorption correction	Multi-scan	Multi-scan
T_{min}, T_{max}	0.833, 1	0.971, 1
No. of measured, independent and observed [$I > 2\sigma(I)$] reflections	118 881, 20 944, 18 223	13 337, 4185, 2285
R_{int}	0.057	0.079
Refinement		
$R[F^2 > 2\sigma(F^2)], wR(F^2), S$	0.039, 0.092, 1.06	0.046, 0.076, 0.82
No. of reflections	20 944	4185
No. of parameters	1188	308
H-atom treatment	All H-atom parameters refined	All H-atom parameters constrained
$\Delta\rho_{max}, \Delta\rho_{min}$ (e Å ⁻³)	0.91, -0.83	0.63, -0.66

 Computer programs used: *CrystalClear-SM* (Rigaku, 2010), *CrysAlis* (Oxford Diffraction Ltd, 2005), *SHELXL97* (Sheldrick, 2008).

In our current work, two novel thermal stable Zn-MOF structures, $Zn_5(\mu_3-OH)(BTC)_3(Phen)_4 \cdot 5H_2O$ (HUT-11), and $Zn_4(\mu_4-O)(BTC)_2(Phen)_2 \cdot 4H_2O$ (HUT-12), are prepared with a similar protocol in the hydrothermal synthesis. Controlling the pH is crucial to obtaining the different crystal structures. HUT-11 contains two kinds of SBUs, $Zn_3(\mu_3-OH)(COO)_5$ clusters and $Zn_2(COO)_4$ clusters. It exhibits a new three-dimensional (3,4,5)-connected topology with the Schläfli symbol $(4 \cdot 6 \cdot 8)_2(4 \cdot 8^2)(4 \cdot 6^4 \cdot 8^5)(4^2 \cdot 6^2 \cdot 8^2)$. HUT-12 is composed of $Zn_4(\mu_4-O)(COO)_6$ clusters as the SBUs and displays a two-dimensional (3,6)-connected TiS_2 related net topology with

obtain white micelles. The use of two Zn metal sources does not give any different crystalline results. The final mixture with a molar ratio of 2 $Zn(OAc)_2$:1 H3BTC:1 Phen:4.8 NaOH for HUT-11 (pH = 7.1) was transferred to stainless steel covered Teflon containers after further stirring for 40 min and then hydrothermally treated at 453 K for 5–7 d. The transparent colourless crystal was collected after washing and drying (*ca* 29% yield for HUT-11 was calculated based on H3BTC). A similar preparation for $Zn_4(\mu_4-O)(BTC)_2(Phen)_2 \cdot 4H_2O$ (HUT-12) was used as for HUT-11, but the sodium content was slightly different to guide the structure. NaOH (8.0 ml, 2 M) was used with the final molar ratio of 2 $Zn(OAc)_2$:1 H3BTC:1 Phen:4 NaOH (pH = 6.7). The transparent colourless crystal was collected after washing and drying (*ca* 58% for HUT-12 was calculated based on H3BTC). X-ray and simulated powder patterns of HUT-11 and HUT-12 are presented in Fig. 1.


Figure 1

(a) Simulated and (b) powder X-ray diffraction patterns of (left) HUT-11 and (right) HUT-12.

the Schläfli symbol $(4^2 \cdot 6)(4^4 \cdot 6^2 \cdot 8^8 \cdot 10)$. Their photoluminescence properties are studied. Metal-to-ligand charge transfer (MLCT) exists in both structures, accompanying a weak metal-centred fluorescence. A red shift is observed in the higher density crystals HUT-11. The additional Phen ligand is helpful in increasing the thermal stability of the frameworks when compared with single ligand MOFs. Both of the two new MOFs show high thermal stability with a decomposition temperature above 673 K in air.

2. Experimental

2.1. Crystal preparation

$Zn_5(\mu_3-OH)(BTC)_3(Phen)_4 \cdot 5H_2O$ (HUT-11) was prepared using the following protocol. 1,3,5-Benzenetricarboxylate (H3BTC) (0.84 g, 4 mmol)/NaOH (9.6 ml, 2 M) water solution (50 ml) was mixed with phenanthroline (Phen) (0.79 g, 4 mmol)/ethanol (10 ml) solution with stirring at room temperature for half an hour. Then $Zn(OAc)_2$ (1.75 g, 8 mmol) or $ZnCl_2$ (1.09 g, 8 mmol) was dropped into the mixture to obtain white micelles. The use of two Zn metal sources does not give any different crystalline results. The final mixture with a molar ratio of 2 $Zn(OAc)_2$:1 H3BTC:1 Phen:4.8 NaOH for HUT-11 (pH = 7.1) was transferred to stainless steel covered Teflon containers after further stirring for 40 min and then hydrothermally treated at 453 K for 5–7 d. The transparent colourless crystal was collected after washing and drying (*ca* 29% yield for HUT-11 was calculated based on H3BTC). A similar preparation for $Zn_4(\mu_4-O)(BTC)_2(Phen)_2 \cdot 4H_2O$ (HUT-12) was used as for HUT-11, but the sodium content was slightly different to guide the structure. NaOH (8.0 ml, 2 M) was used with the final molar ratio of 2 $Zn(OAc)_2$:1 H3BTC:1 Phen:4 NaOH (pH = 6.7). The transparent colourless crystal was collected after washing and drying (*ca* 58% for HUT-12 was calculated based on H3BTC). X-ray and simulated powder patterns of HUT-11 and HUT-12 are presented in Fig. 1.

2.2. Characterization

X-ray powder diffraction (XRPD) patterns were recorded on a Rigaku D/Max 2500 diffractometer using $Cu K\alpha$ radiation running at a voltage

of 40 kV and a current of 30 mA. Fourier-transform IR radiation (FT-IR) was recorded on a Thermo Nicolet Nexus 470 with KBr tablet at room temperature. The narrow $\nu(\text{OH})$ bands at 3469 and 3368 cm^{-1} are associated with the existence of strong hydrogen bonds. Stretching bands characteristic of the carboxylic group were located at 1643 and 1620 cm^{-1} . The intense bands centred at 1352, 1426 and 1576 cm^{-1} were attributed to the stretching vibration of $\text{C}=\text{O}$ ($\nu\text{C}=\text{O}$), $\text{C}=\text{C}$ ($\nu\text{C}=\text{C}$) and $\text{C}-\text{H}$ ($\nu\text{C}-\text{H}$) groups. Differential scanning calorimetry and thermogravimetric analysis (DSC-TGA) was performed on an AC TG-DTA SDT Q600 V20.9 apparatus in an aluminium pan. The sample was heated to 873 K in air with

a heating rate of 5 K min^{-1} . The steady-state luminescence spectra was measured on an Edinburgh Instruments FS920P spectrometer, with a 450 W xenon lamp as the steady-state excitation source, a double excitation monochromator (1800 lines mm^{-1}), an emission monochromator (600 lines mm^{-1}), and a semiconductor cooled Hamamatsu RMP928 photomultiplier tube. Single-crystal X-ray diffraction data were collected for HUT-11 at Diamond Light Source, beamline I19 at 150 K on a Rigaku Saturn 724+ CCD diffractometer with $\lambda = 0.6889 \text{ \AA}$. Data integration and numerical absorption correction were carried out by the *d*TREK* software package from Rigaku (Pflugrath, 1999). Single-crystal X-ray diffraction data were collected for HUT-12 at room temperature on an Oxford Diffraction Xcalibur CCD diffractometer with Mo $K\alpha$ radiation ($\lambda = 0.71073 \text{ \AA}$). Data integration and numerical absorption correction were carried out by the *CrysAlis* software package from Oxford Diffraction Ltd (2005). Structure refinements for both HUT-11 and HUT-12 were made with the *SHELXL* program package using the interface *WinGX* (Farrugia, 1999).

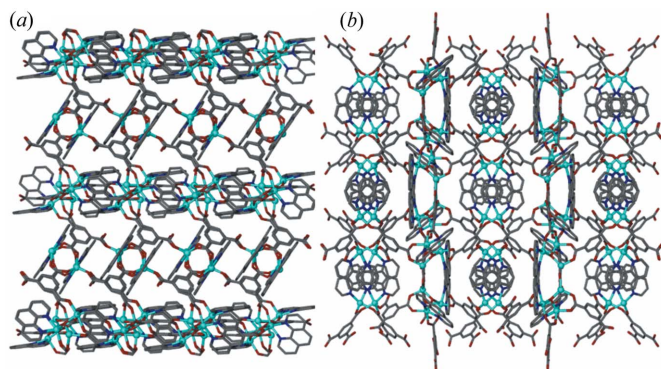


Figure 2
(a) and (b) structure views along the *b* axis and *c* axis for HUT-11 (Zn: cyan, O: red, N: blue, C: grey).

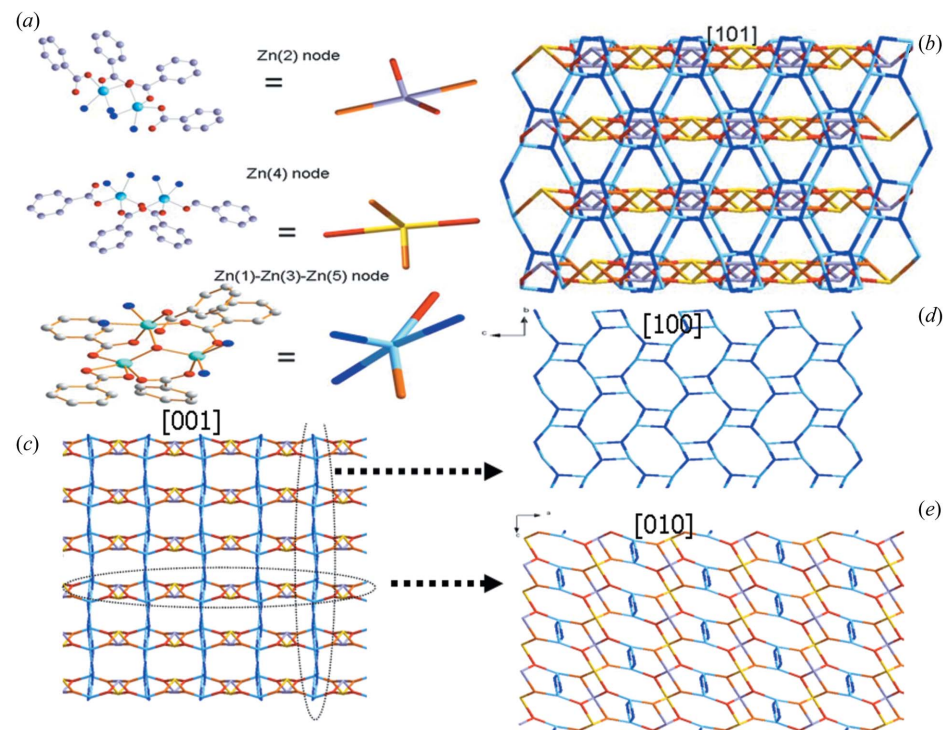


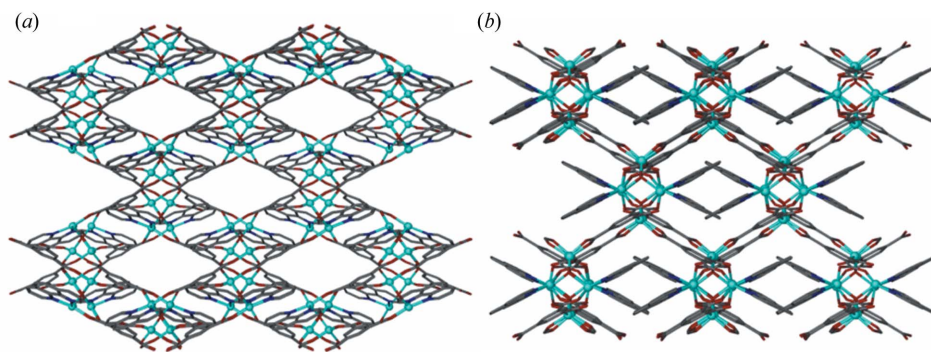
Figure 3
(a) Zn (2), Zn (4) and $\text{Zn}_3(\mu_3\text{-OH})$ clusters in HUT-11 with grey, yellow and cyan. (b) and (c) the topology images viewed along [101] and [001] axes. (d) and (e) the separated plane along the *a* and *b* axes.

3. Results and discussion

3.1. Crystal structure

Single-crystal data revealed, by analyzing systematic reflection absences, that the two MOFs crystallize in the same space group $C2/c$ (No.15; Table 1). In HUT-11 (Figs. 2 and 3) the asymmetric unit consists of five unique Zn atoms, four

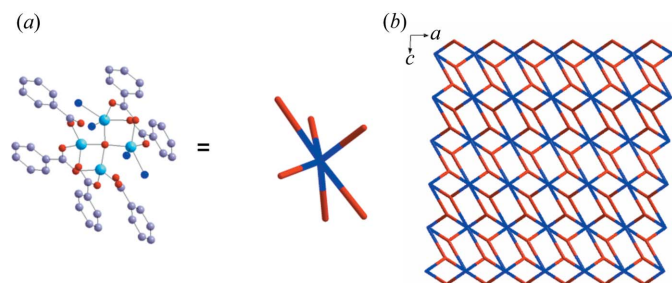
Phen molecules and three molecules of BTC. The $\text{Zn}_3(\mu_3\text{-OH})$ core is composed of Zn1 (six-coordination), Zn3 (five-coordination) and Zn5 (five-coordination) bridged by a $\mu_3\text{-OH}$ unit in a co-planar arrangement (Fig. 3a). The trinuclear basic building unit is formed due to the bridging carboxylate groups from five distinctive ligands binding three zinc atoms with a $\mu_3\text{-OH}$ at the centre. Similar trinuclear SBUs have been reported in $\text{Zn}_6(\mu_3\text{-OH})_2(L)_2(\text{H}_2\text{O})_{6n}$ structure, where $L = 1,2,3,4,5\text{-benzenepentacarboxylate}$ (Wang *et al.*, 2008), and in the three-dimensional framework $\text{Zn}_3(\text{BDC})_3 \cdot 6\text{CH}_3\text{OH}$ (BDC = 1,4-benzenedicarboxylate) in which the three zinc centres are arranged linearly with an inversion centre on Zn1 (Eddaoudi *et al.*, 2000). Meanwhile, the bimetallic Zn2 and Zn4 clusters are formed which connect to two Phens and two BTCs, respectively, giving rise to $\pi\text{-}\pi$ interactions between their


Figure 4

Structure of HUT-12 along (a) the c axis and (b) the $[101]$ direction. Colour code for (b) and (c): Zn: cyan, O: red, N: blue, C: grey.

connected aryl rings (Mahata & Natarajan, 2009). Amongst five-coordinated Zn ions, Zn3, Zn4 and Zn5 present trigonal bipyramid polyhedrons. Only Zn2 adopts a square-pyramid polyhedron, which causes the structure to have lower symmetry compared with the reported similar structure (Wang *et al.*, 2008). A better approach to obtain insight into the essence of the complex framework can be achieved by a topology study. The three-dimensional-(3,4,5)-connected Schläfli symbol is calculated as $(4\cdot6\cdot8)_2(4\cdot8^2)(4\cdot6^4\cdot8^5)(4^2\cdot6^2\cdot8^2)$ (Fig. 3). This structure has two perpendicular layers along the a and b axes. Five coordinated Zn1–Zn3–Zn5 nodes are the cross points in the two planes. Thus, the topology of HUT-11 can be described as two sets of perpendicular layers, along the $[100]$ and $[101]$ axes (Figs. 3*d* and *e*), which cross and share common four-membered rings.

In HUT-12 there are two unique Zn atoms, one molecule BTC and one molecule Phen per formula unit (Fig. 4). The Zn metal ions have two types of coordination sites. Zn1 is tetrahedrally coordinated and is connected to three BTCs. Zn2 is trigonal bipyramidally coordinated and is connected to two BTCs and one Phen, which is much simpler compared with HUT-11. HUT-12 adopts a neutral $Zn_4O(COO)_6$ cluster. It contains two Zn1 and two Zn2 atoms with a shared O atom. Each Zn pair is connected by the *syn-syn* carboxylate O atom. The structure along the $[101]$ direction is equally partitioned with four phenanthroline molecules to form a small parallel


Figure 5

(a) Representation of the distorted octahedral node of the Zn cluster linked to six BTC units; (b) schematic illustration of the (3,6)-connected net along the b axis based on TiS_2 -related topology of HUT-12. Colour code: red for three-connected BTC ligands; blue for Zn octahedral SBUs.

logram (Fig. 4). Likewise, BTC ligands are defined as three-connected nodes. Therefore, it can be clearly shown along the a axis that the three-dimensional (3,6)-connected net topology is signified with the Schläfli symbol $(4^2\cdot6)(4^4\cdot6^2\cdot8^8\cdot10)$ (Fig. 5). Herein, the structure based on $Zn_4(\mu_4-O)(COO)_6$ clusters adopts the TiS_2 -related topology and is different from the reported (3,6)-connected MOFs (Su *et al.*, 2009; Mahata & Natarajan, 2009; Zou *et al.*, 2010).

The structure of HUT-11 and HUT-12 are formed as the Zn^{II}

ions adopt different connection modes with the effect of Phen and H3BTC. Several factors have been taken into consideration in the rational design of MOF structures. These factors include not only the properties of both organic and inorganic units, such as coordination ability and steric hindrance of organic ligands, and the electronic structure of metal ions (Wang *et al.*, 2006; Xiao *et al.*, 2007), but also the conditions employed in the preparation, including reacting temperature, time, pH value and the ratio of reactants (Forster, *et al.*, 2005; Cheetham *et al.*, 2006). In our work the only difference between HUT-11 and HUT-12 is the pH value, *i.e.* the H3BTC/NaOH ratio, which leads to entirely different connectivity modes of H3BTC in the two structures. Our preparation shows that the charged $Zn_3(\mu_3-OH)$ cluster is obtained at higher pH values. Fig. 6 shows the three coordination modes observed in HUT-11 and HUT-12. To the best of our knowledge, the coordination modes of Fig. 6(c) have not been reported despite the fact that Zn–H3BTC MOFs have been studied extensively (Xu *et al.*, 2007).

It is well known that the hydrothermal system conditions, such as the ratio of the initial composition, temperature and pH value, are found to be crucial to the crystal structure, crystallization and purity of the products. For example, Co-MOFs can be prepared in acidic media making a complex between Co and two $RCOO^-$ groups to form a linear polymer, whereas at neutral pH all the initial water molecules have been displaced by succinate ions and the prepared $Co_4(OH)_2(H_2O)_2(C_4H_4O_4)_3\cdot 2H_2O$ gives corrugated layers (Livage *et al.*, 2001). Both Zn–O and Zn–N bonds are found in this system due to the use of BTC and Phen. It cannot be said if the use of two different ligands makes the synthesis more sensitive towards pH, although it has been observed that a small change in NaOH content gives a large effect on the synthesized crystal structure. The structures of HUT-11 and HUT-12 are formed at pH = 7.1 and pH = 6.7, respectively. Concerning their structures, HUT-11 has μ_3-OH to charge balance the framework and HUT-12 has a neutral structure. This implies that a less acidic system may lead to the charged framework. However, more studies on the effect of NaOH

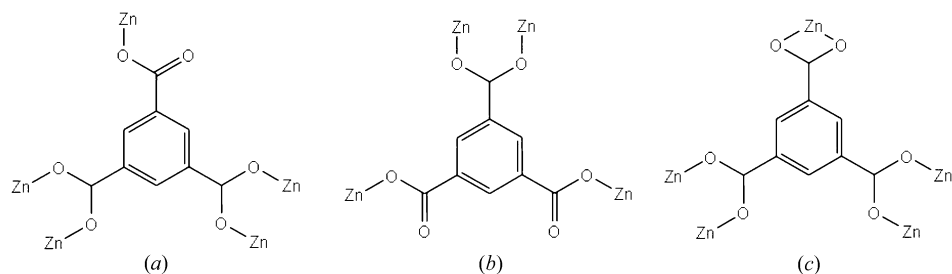


Figure 6
Coordination mode of the BTC ligand in HUT-11 (a), (b) and (c) and HUT-12 (a).

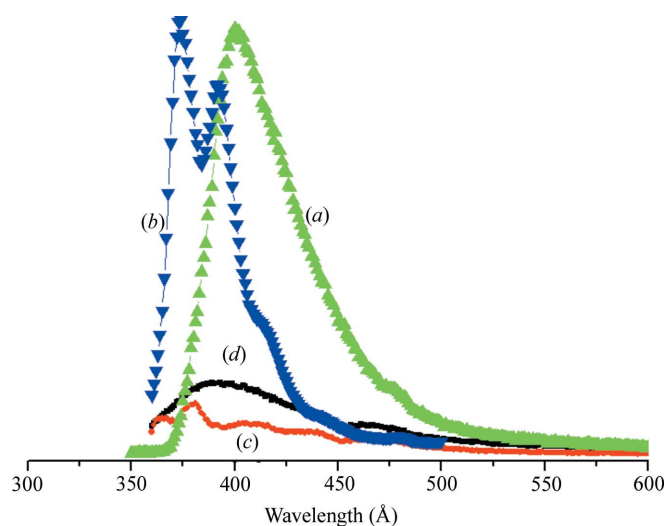


Figure 7
Photoluminescence spectra of (a) HUT-11, (b) HUT-12, (c) Phen and (d) H3BTC ($\lambda_{ex} = 330$ nm).

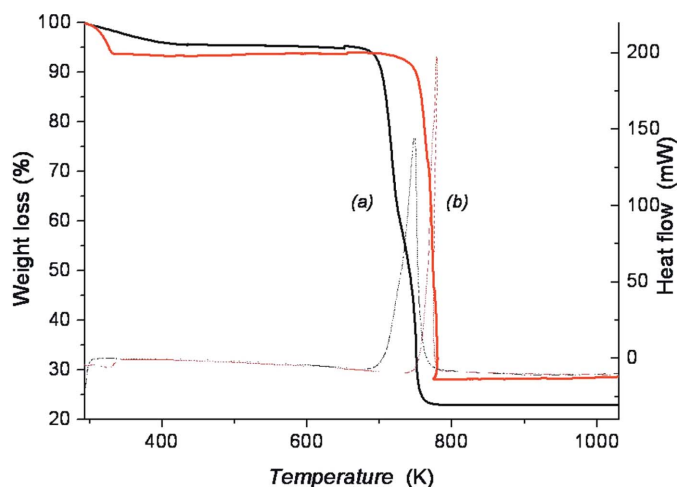


Figure 8
DSC-TGA curves of (a) HUT-11 and (b) HUT-12 in air flow with rate of 5 K min^{-1} .

should be carried out in order to examine its control on the crystal growth.

3.2. Crystal properties

Photoluminescence studies (Fig. 7) showed that the excitation of the solid HUT-11 and HUT-12 at 280 nm produces a luminescence peak in the range 374–400 nm. As the emissions of the two materials are very similar to the free H3BTC ligand located at 370 nm and Phen at ca 390 nm (Fang *et al.*, 2006; Fu *et al.*, 2002), they may be ligand-centred electronic transitions perturbed by the coordination to metal ions rather than to protons. Meanwhile, these two Zn-MOFs show clearly the effect of the framework density and coordination environment of Zn clusters, which lead to the difference in their photoluminescence behaviour (Ngan *et al.*, 2007; Chen *et al.*, 2003).

Differential scanning calorimetric and thermogravimetric analysis (DSC-TGA) was performed on a TA SDT Q600 apparatus in an aluminium pan. The sample was heated to 873 K in air with a heating rate of 5 K min^{-1} . As shown in Fig. 8, HUT-11 ($\text{Zn}_5(\mu_3\text{-OH})(\text{BTC})_3(\text{Phen})_4 \cdot 5\text{H}_2\text{O}$) and HUT-12 ($\text{Zn}_4(\mu_4\text{-O})(\text{BTC})_2(\text{Phen})_2 \cdot 4\text{H}_2\text{O}$) have the majority of the weight loss occurring above 373 K. The weight loss below 373 K is due to the loss of crystal water. The main weight losses of 77% in HUT-11 at 748 K and 72% in HUT-12 at 773 K indicate that the framework starts to collapse with the loss of BTC and Phen at the same time. According to the molecular formulae of HUT-11 and HUT-12 the residue weight of ZnO after calcination should be 22.54 and 28.96%. The TGA study is consistent with these calculations.

In order to confirm the thermal stability of two compounds, calcinations in a muffle oven were performed at different temperatures, and the corresponding XRD patterns are shown in Fig. 9. It is observed that HUT-11 keeps its structure well to 673 K, but changes into ZnO powder (PCPDF 65–3411) at 748 K. HUT-12 is more stable than HUT-11, which keeps its structure at 723 K but decomposes into white ZnO powder (PCPDF 65–3411) at 773 K. This is in accordance with the TGA observation. Also, the higher thermal stability of HUT-12 suggests that the higher density is helpful to strengthen the framework.

4. Conclusions

Two new coordination Zn-MOFs with different architectures have been synthesized and characterized using the binary ligand system 1,3,5-benzenetricarboxylic acid and phenanthroline by controlling the condition of hydrothermal systems. Compounds HUT-11 and HUT-12 are three-dimensional coordination frameworks constructed with different SBUs of metal-carboxylate clusters. Two novel coordination modes between the Zn metal and carboxylate are observed in the

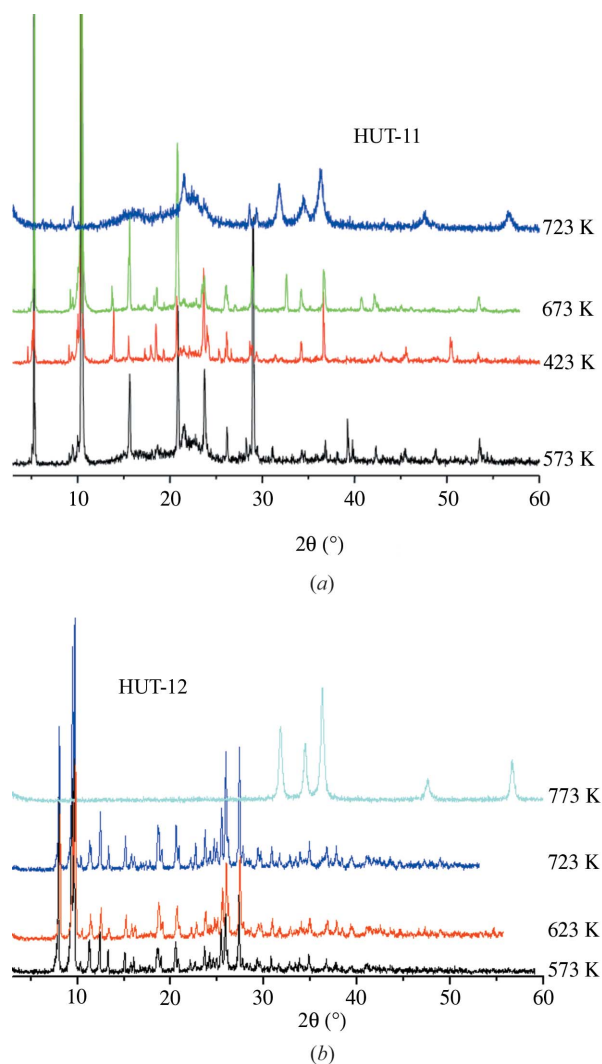


Figure 9

XRD patterns of thermal treated sample (a) HUT-11 and (b) HUT-12 in muffle oven with 5 K min^{-1} and kept 30 min at each sample point in atmosphere.

structures presented here. The results reveal that the adjustment of the alkaline source in the hydrothermal system plays an important role in the structural arrangement. Both crystals possess high thermal stability above 673 K.

This work was supported by the National Natural Science Foundation of China (20803017), Key Project of Chinese

Ministry of Education (2009CB623502), Ph.D. Programs Foundation of Ministry of Education of China (20091317120005), and Scientific Research Foundation for the Returned Overseas Chinese Scholars, State Education Ministry. We also thank Diamond Light Source for beamtime at Beamline I19.

References

- Cheetham, A. K., Rao, C. N. R. & Feller, R. K. (2006). *Chem. Commun.* pp. 4780–4795.
- Chen, W., Wang, J. Y., Chen, C., Yue, Q., Yuan, H. M., Chen, J. S. & Wang, S. N. (2003). *Inorg. Chem.* **42**, 944–946.
- Cui, Y., Evans, O. R., Ngo, H. L., White, P. S. & Lin, W. B. (2005). *Angew. Chem. Int. Ed.* **41**, 1159–1162.
- Eddaoudi, M., Li, H. & Yaghi, O. M. (2000). *J. Am. Chem. Soc.* **122**, 1391–1397.
- Fang, Q. R., Zhu, G. S., Jin, Z., Xue, M., Wei, X., Wang, D. J. & Qiu, S. L. (2007). *Cryst. Growth Des.* **7**, 1035–1037.
- Fang, Q., Zhu, G., Xue, M., Sun, J., Sun, F. & Qiu, S. (2006). *Inorg. Chem.* **45**, 3582–3587.
- Farrugia, L. J. (1999). *J. Appl. Cryst.* **32**, 837–838.
- Forster, P. M., Stock, N. & Cheetham, A. K. (2005). *Angew. Chem. Int. Ed.* **44**, 7608–7611.
- Fu, Z. Y., Wu, X. T., Dai, J. C., Hu, S. M., Du, W. X., Zhang, H. H. & Sun, R. Q. (2002). *Eur. J. Inorg. Chem.* **41**, 2730–2735.
- Li, J. R., Tao, Y., Yu, Q. & Bu, X. H. (2007). *Chem. Commun.* pp. 1527–1529.
- Livage, C., Egger, C. & Férey, G. (2001). *Chem. Mater.* **13**, 410–414.
- Mahata, P. & Natarajan, S. (2009). *CrystEngComm*, **11**, 560–563.
- Ngan, T. W., Ko, C. C., Zhu, N. & Yam, V. W. (2007). *Inorg. Chem.* **46**, 1144–1152.
- Oxford Diffraction Ltd (2005). *CrysAlis*, Version 1.171.32. Oxford Diffraction Ltd, Abingdon, England.
- Pflugrath, J. W. (1999). *Acta Cryst. D* **55**, 1718–1725.
- Rigaku (2010). *CrystalClear Expert 2.0 r5*. Rigaku Corporation, Tokyo, Japan.
- Rosi, N. L., Kim, J., Eddaoudi, M., Chen, B., O’Keeffe, M. & Yaghi, O. M. (2005). *J. Am. Chem. Soc.* **127**, 1504–1518.
- Sheldrick, G. M. (2008). *Acta Cryst. A* **64**, 112–122.
- Su, Z., Xu, J. F. J. L. D., Chu, Q., Chen, M., Chen, S., Liu, G., Wang, X. & Sun, W. (2009). *Cryst. Growth Des.* **9**, 2801–2811.
- Wang, J., Lin, Z., Ou, Y. C., Yang, N. L., Zhang, Y. H. & Tong, M. L. (2008). *Inorg. Chem.* **47**, 190–199.
- Wang, X. L., Qin, C., Wang, E. B. & Su, Z. M. (2006). *Chem. Eur. J.* **12**, 2680–2691.
- Xiao, D. R., Li, Y. G., Wang, E. B., Fan, L. L., An, H. Y., Su, Z. M. & Xu, L. (2007). *Inorg. Chem.* **46**, 4158–4166.
- Xu, L., Choi, E. Y. & Kwon, Y. U. (2007). *Inorg. Chem.* **46**, 10670–10680.
- Zou, J., Peng, Q., Wen, Z., Zeng, G., Xing, Q. & Guo, G. (2010). *Cryst. Growth Des.* **10**, 2613–2619.